



UNIVERSITY OF LEEDS

This is a repository copy of *Accounting for Changing Temperature Patterns Increases Historical Estimates of Climate Sensitivity*.

White Rose Research Online URL for this paper:
<http://eprints.whiterose.ac.uk/137122/>

Version: Accepted Version

Article:

Andrews, T, Gregory, JM, Paynter, D et al. (7 more authors) (2018) Accounting for Changing Temperature Patterns Increases Historical Estimates of Climate Sensitivity. *Geophysical Research Letters*, 45 (16). pp. 8490-8499. ISSN 0094-8276

<https://doi.org/10.1029/2018GL078887>

© 2018 Crown copyright. This article is published with the permission of the Controller of HMSO and the Queen's Printer for Scotland. This is the peer reviewed version of the following article: Andrews, T, Gregory, JM, Paynter, D et al. (7 more authors) (2018) Accounting for Changing Temperature Patterns Increases Historical Estimates of Climate Sensitivity. *Geophysical Research Letters*, 45 (16). pp. 8490-8499, which has been published in final form at <https://doi.org/10.1029/2018GL078887>. This article may be used for non-commercial purposes in accordance with Wiley Terms and Conditions for Use of Self-Archived Versions.

Reuse

Items deposited in White Rose Research Online are protected by copyright, with all rights reserved unless indicated otherwise. They may be downloaded and/or printed for private study, or other acts as permitted by national copyright laws. The publisher or other rights holders may allow further reproduction and re-use of the full text version. This is indicated by the licence information on the White Rose Research Online record for the item.

Takedown

If you consider content in White Rose Research Online to be in breach of UK law, please notify us by emailing eprints@whiterose.ac.uk including the URL of the record and the reason for the withdrawal request.



eprints@whiterose.ac.uk
<https://eprints.whiterose.ac.uk/>

1 Accounting for changing temperature patterns 2 increases historical estimates of climate sensitivity

3

4 Timothy Andrews^{1#}, Jonathan M. Gregory^{1,2}, David Paynter³, Levi G. Silvers⁴, Chen Zhou⁵,
5 Thorsten Mauritsen⁶, Mark J. Webb¹, Kyle C. Armour⁷, Piers M. Forster⁸ and Holly Titchner¹.

6

7 ¹Met Office Hadley Centre, Exeter, UK.

8 ²NCAS-Climate, University of Reading, Reading, UK.

9 ³GFDL-NOAA, Princeton, USA.

10 ⁴Princeton University / GFDL, Princeton, USA.

11 ⁵Nanjing University, China.

12 ⁶Max Planck Institute for Meteorology, Hamburg, Germany.

13 ⁷University of Washington, Seattle, USA.

14 ⁸School of Earth and Environment, University of Leeds, Leeds, UK.

15

16 Submitted: 23rd May 2018

17 Revised: 10th July 2018

18 Key points

- 19
- Climate sensitivity simulated for observed surface temperature change is smaller
20 than for long-term carbon dioxide increases.
 - Observed historical energy budget constraints give climate sensitivity values that are
21 too low and overly constrained, particularly at the upper end.
 - Historical energy budget changes only weakly constrain climate sensitivity.
- 22
23
24

25

26 [#]Corresponding Author:

27 Timothy Andrews

28 Met Office Hadley Centre

29 FitzRoy Road

30 Exeter, EX1 3PB.

31 E-mail: timothy.andrews@metoffice.gov.uk

32 Abstract

33 Eight Atmospheric General Circulation Models (AGCMs) are forced with observed historical
34 (1871-2010) monthly sea-surface-temperature (SST) and sea-ice variations using the AMIP
35 II dataset. The AGCMs therefore have a similar temperature pattern and trend to that of
36 observed historical climate change. The AGCMs simulate a spread in climate feedback
37 similar to that seen in coupled simulations of the response to CO₂ quadrupling. However the
38 feedbacks are robustly more stabilizing and the effective climate sensitivity (EffCS) smaller.
39 This is due to a 'pattern effect' whereby the pattern of observed historical SST change gives
40 rise to more negative cloud and LW clear-sky feedbacks. Assuming the patterns of long-
41 term temperature change simulated by models, and the radiative response to them, are
42 credible, this implies that existing constraints on EffCS from historical energy budget
43 variations give values that are too low and overly constrained, particularly at the upper end.
44 For example, the pattern effect increases the long-term Otto et al. (2013) EffCS median and
45 5-95% confidence interval from 1.9K (0.9-5.0K) to 3.2K (1.5-8.1K).

46 Plain text summary

47 Recent decades have seen cooling over the eastern tropical Pacific and Southern Ocean
48 while temperatures rise globally. Climate models indicate that these regional features, and
49 others, are not expected to continue into the future under sustained forcing from atmospheric
50 carbon dioxide increases. This matters, because climate sensitivity depends on the pattern
51 of warming, so if the past has warmed differently from what we expect in the future then
52 climate sensitivity estimated from the historical record may not apply to the future. We
53 investigate this with a suite of climate models and show that climate sensitivity simulated for
54 observed historical climate change is smaller than for long-term carbon dioxide increases.
55 The results imply that historical energy budget changes only weakly constrain climate
56 sensitivity.

57 1. Introduction

58 The relationship between global surface temperature change and the Earth's radiative
59 response - a measure of the radiative feedbacks in the system and a key determinant of the
60 Earth's climate sensitivity - can vary on timescales of decades to millennia. Thus feedbacks
61 governing warming over the observed historical record may be different from those acting on
62 the Earth's long-term climate sensitivity to rising greenhouse gas concentrations (e.g.
63 Gregory and Andrews 2016; Zhou et al., 2016; Armour 2017; Proistosescu and Huybers
64 2017; Silvers et al., 2018; Marvel et al., 2018). This is in contrast to decades of studies that
65 explicitly or implicitly assume that the relationship between historical temperature change
66 and energy budget variations provides a direct constraint on long-term climate sensitivity
67 (e.g. Gregory et al., 2002; Otto et al., 2013).

68
69 The primary reason why radiative feedback and sensitivity is not constant is because climate
70 feedback depends on the spatial structure of surface temperature change (Armour et al.
71 2013; Rose et al., 2014; Andrews et al., 2015; Zhou et al. 2016; 2017; Haugstad et al., 2017;
72 Ceppi and Gregory, 2017; Andrews and Webb, 2018; Silvers et al., 2018). This evolves on
73 annual to decadal timescales with modes of unforced coupled atmosphere-ocean variability
74 (e.g. Xie et al., 2016) and spatiotemporal variations in anthropogenic or natural forcings (e.g.
75 Takahashi and Watanabe, 2016; Smith et al., 2016). It also evolves on decadal to
76 centennial timescales in response to sustained anthropogenic forcing due to the intrinsic
77 timescales of the climate response (such as delayed warming in the eastern tropical Pacific
78 and Southern Ocean) (e.g. Senior and Mitchell, 2000; Andrews et al., 2015; Armour et al.,
79 2016). Thus the pattern of historical temperature change, and thus radiative feedback, is
80 expected to be different from that in response to long-term CO₂ increases (see Discussion).
81 We refer to the dependency of radiative feedbacks on the evolving pattern of surface
82 temperature change as a 'pattern effect' (Stevens et al., 2016).

83
84 Most previous estimates of climate sensitivity based upon historical observations of Earth's
85 energy budget have not allowed for a pattern effect between historical climate change and
86 the long-term response to CO₂ (e.g. Otto et al., 2013). Armour (2017) found that the
87 equilibrium climate sensitivity (ECS) (the equilibrium near surface-air-temperature change in
88 response to a CO₂ doubling) of Atmosphere-Ocean General Circulation Models (AOGCMs)
89 (estimated from simulations of abrupt CO₂ quadrupling (abrupt-4xCO₂)) was about 26%
90 larger than climate sensitivity inferred from transient warming (1%CO₂ simulations, taken to
91 be an analogue for historical climate change) due to pattern effects. Armour (2017)

92 therefore concluded that energy budget estimates of Earth's ECS from the historical record
93 should be increased by this amount. Lewis and Curry (2018) argue for a smaller pattern
94 effect, highlighting ambiguities in the methodology when using idealised CO₂ experiments as
95 an analogue for historical climate change. However, as noted in Armour (2017), the use of
96 1%CO₂ simulations as an analogue for historical climate change has important limitations in
97 that it neglects the impact from non-CO₂ forcings and unforced climate variability that could
98 have had a significant impact on the pattern of historical temperature change. In particular,
99 under 1%CO₂, AOGCMs do not show cooling of the tropical eastern Pacific Ocean and
100 Southern Ocean – features that have been observed over recent decades but are not
101 expected in the long-term response to increased CO₂ (Zhou et al., 2016). These are regions
102 where atmospheric feedbacks (in particular clouds) are sensitive to the patterns of surface
103 temperature change due to their impact on local and remote atmospheric stability (e.g. Zhou
104 et al., 2017; Andrews and Webb, 2018). This suggests that the magnitude of the pattern
105 effect reported in Armour (2017) may be too low relative to historical climate change. This is
106 an outstanding issue that we aim to address and quantify here.

107

108 Here we will show that a suite of Atmospheric General Circulation Models (AGCMs) forced
109 with historical (post 1870) sea-surface-temperatures (SSTs) and sea-ice changes are ideal
110 simulations for quantifying the relationship between historical climate sensitivity and
111 idealised long-term model derived ECS. They allow us, for the first time, to quantify the
112 pattern effect associated with observed temperature patterns, and so provide improved
113 updates to estimates of climate sensitivity derived from historical energy budget constraints.
114 The work builds upon individual studies (Andrews, 2014; Gregory and Andrews 2016; Zhou
115 et al., 2016; Silvers et al., 2018). Our aim is to: (i) bring together these individual model
116 results for an intercomparison of AGCMs forced with historical SST and sea-ice variations;
117 (ii) explore the dependence of the experimental design to the underlying SST and sea-ice
118 dataset; (iii) explore how historical feedbacks in the AGCMs relate to feedbacks diagnosed
119 from their parent AOGCM forced by abrupt-4xCO₂; (iv) quantify the pattern effect causing
120 the difference between climate sensitivity under historical climate change and long-term CO₂
121 changes; (v) use this pattern effect to update observed energy budget constraints on Earth's
122 climate sensitivity.

123 2. Simulations, Models and Data

124 Eight AGCMs (Table 1) are forced with monthly time-varying observationally derived fields of
125 SST and sea-ice from 1871 to 2010 using the Atmospheric Model Intercomparison Project

126 (AMIP) II boundary condition data set (Gates et al., 1999; Taylor et al., 2000; Hurrell et al.,
127 2008). All simulations have natural and anthropogenic forcings (e.g. greenhouse gases,
128 aerosols, solar radiation etc.) held constant at assumed pre-industrial conditions (except
129 CAM4 which used assumed constant present-day conditions; we assume the level of
130 background forcing has no impact on the diagnosed feedback of the model). With constant
131 forcings the variation in radiative fluxes comes about solely from the changing SST and sea-
132 ice boundary conditions, allowing radiative feedbacks to be accurately diagnosed directly
133 from top-of-atmosphere (TOA) radiation fields (e.g. Haugstad et al., 2017). For details of
134 individual simulations see Gregory and Andrews (2016) for HadGEM2 and HadAM3, Silvers
135 et al. (2017) for GFDL-AM2.1, GFDL-AM3 and GFDL-AM4.0, Zhou et al. (2016) for CAM4
136 and CAM5.3, and Mauritsen et al. (2018) for ECHAM6.3. This experiment, referred to here
137 as amip-piForcing (Gregory and Andrews, 2016), is included in the Cloud Feedback Model
138 Intercomparison Project (CFMIP) contribution to CMIP6 (Webb et al. 2017). The sensitivity
139 of the results to the AMIP II boundary condition dataset is explored with analogous
140 experiments using the HadISST2.1 SST and sea-ice dataset (Titchner and Rayner, 2014)
141 (Supporting Information).

142
143 All simulations ran for 140yrs from Jan 1871 through to Dec 2010, except for GFDL-AM2.1
144 and GFDL-AM3 which finished in Dec 2004. All data is global-annual-mean and anomalies
145 are presented relative to an 1871-1900 baseline. CAM4 and CAM5.3 results are single
146 realisations, HadGEM2 and HadAM3 simulations are ensembles of 4 realisations each,
147 ECHAM6.3, GFDL-AM2.1 and GFDL-AM4.0 have 5 realisations each, while GFDL-AM3 has
148 6 realisations. The HadGEM2 results are not identical to those presented in Gregory and
149 Andrews (2016) because it has been discovered that land-cover change was included in
150 their HadGEM2 simulations. We have confirmed that the updated simulations used here,
151 which have constant land-cover, do not affect the main conclusions of Gregory and Andrews
152 (2016). In fact the multi-decadal variability in feedback in HadGEM2 is now found to be more
153 consistent with their HadAM3 results (Section 3).

154
155 For comparison to long-term climate sensitivity and feedback parameters we make use of an
156 abrupt-4xCO₂ simulation of each AGCM's parent AOGCM. For CAM4, GFDL-AM2.1,
157 GFDL-AM3 and HadGEM2 we use the CCSM4, GFDL-ESM2M, GFDL-CM3 and HadGEM2-
158 ES CMIP5 abrupt-4xCO₂ simulations respectively (Taylor et al., 2012). Feedbacks and
159 associated effective climate sensitivity (EffCS) (the equilibrium near surface-air-temperature
160 change in response to a CO₂ doubling assuming constant feedback strength) are derived
161 from the regression of global-annual-mean change in radiative flux dN against surface-air-
162 temperature change dT for the 150yrs of the simulation, according to $\text{EffCS} = -F_{2x}/\lambda$, where

163 F_{2x} , the forcing from a doubling of CO_2 , is equal to the dN-axis intercept divided by two (to
 164 convert $4xCO_2$ to $2xCO_2$) and λ , the feedback parameter, is equal to the slope of the
 165 regression line (Andrews et al., 2012). We have similar simulations for ECHAM6.3 and
 166 HadAM3 using the MPI-ESM1.1 and HadCM3 models respectively, though these are not in
 167 the CMIP5 archive. The HadCM3 simulation is only 100yrs long but is a mean of 7
 168 realisations. CAM5.3 and GFDL-AM4.0 do not yet have equivalent coupled $4xCO_2$
 169 simulations. We choose to use EffCS rather than the ‘true’ equilibrium climate sensitivity
 170 (ECS) since few AOGCMs are run to equilibrium and thus the true ECS is not generally
 171 known. Paynter et al. (2018) showed that the actual ECS from multimillennial GFDL-
 172 ESM2M and GFDL-CM3 simulations was nearly 1K higher than the EffCS we use here from
 173 abrupt- $4xCO_2$. Hence the values we report for EffCS might be viewed as a lower bound on
 174 ECS if other models behave in a similar way.

175 3. Radiative feedbacks and sensitivities

176 Figure 1a shows the global-annual-mean near-surface-air-temperature change (dT) of the
 177 eight individual AGCM amip-piForcing simulations in comparison to HadCRUT4 (Morice et
 178 al., 2012). As expected the models capture the observed variability and trends in dT well (the
 179 correlation coefficient, r , between observed and simulated dT is >0.95 for every model).
 180 However the AGCMs omit the small part of the recent warming trend over land that arises as
 181 a direct adjustment to changes in CO_2 and other forcing agents (dT in HadCRUT4 averaged
 182 over 2000-2010 is 0.79K, whereas it ranges from 0.66-0.76K in the AGCMs) (see also,
 183 Andrews, 2014; Gregory and Andrews, 2016). Figure 1b shows the net TOA radiative flux
 184 change, dN. It is generally negative because as dT increases positively the planet loses heat
 185 to space. This relationship is shown in Figure 1c for the multi-model ensemble-mean. The
 186 slope of the regression line (ordinary least-squares, over the annual-mean 1871-2010
 187 timeseries data) measures the feedback parameter λ_{amip} (in $Wm^{-2} K^{-1}$), where subscript
 188 ‘amip’ is used to indicate that the feedback parameter was derived from the amip-piForcing
 189 experiment. Individual model results are given in Table 1.

190
 191 The equivalent feedback parameters derived from six available parent AOGCM abrupt-
 192 $4xCO_2$ simulations (λ_{4xCO_2}) are compared to λ_{amip} in Figure 2 and Table 1. We find that λ_{amip}
 193 is more negative than λ_{4xCO_2} in all models. In other words, AGCMs forced with historical SST
 194 and sea-ice changes robustly simulate more stabilizing feedbacks (lower EffCS) than their
 195 parent AOGCM forced by long-term CO_2 changes. On average, the difference in λ between

196 amip-piForcing and abrupt-4xCO2 is $\Delta\lambda = \lambda_{4xCO2} - \lambda_{amip} = 0.64 \text{ Wm}^{-2} \text{ K}^{-1}$, ranging from 0.29 to
 197 $1.04 \text{ Wm}^{-2} \text{ K}^{-1}$ across the AGCMs (Table 1).

198

199 The source of $\Delta\lambda$ is shown in Figure 2. The clear-sky feedback (Figure 1d,e) is slightly (but
 200 robustly) more negative in amip-piForcing compared to abrupt-4xCO2 (Figure 2b) due to
 201 differences in LW clear-sky feedback processes that are partly offset by SW clear-sky
 202 feedback differences (Figure 2d). This difference in clear-sky alone explains the relatively
 203 small change in net sensitivity for the GFDL-AM2.1 model. For the other models, differences
 204 in cloud feedback (Figure 1f) are a larger source of the reduced sensitivity in amip-piForcing
 205 (Figure 2c). This mostly comes from SW cloud feedback processes, with historical LW cloud
 206 feedback processes generally being representative of that seen in abrupt-4xCO2 (Figure
 207 2e). These findings are consistent with process orientated studies that suggest lapse-rate
 208 (which affects LW clear-sky) and low-cloud (which affect SW and NET CRE) feedbacks vary
 209 the most with SST patterns, especially in the Pacific (see below and: Rose et al., 2014;
 210 Andrews et al., 2015; Zhou et al., 2016; 2017; Silvers et al., 2017; Ceppi and Gregory, 2017;
 211 Andrews and Webb, 2018).

212

213 In amip-piForcing the model-mean $\text{EffCS}_{amip} = -F_{2x} / \lambda_{amip}$ is $\sim 2\text{K}$, ranging from 1.6 to 2.2K
 214 across the AGCMs (Table 1). The narrowness of this EffCS_{amip} range does not arise due to
 215 reduced uncertainty in λ_{amip} relative to λ_{4xCO2} . On the contrary, the spread (measured by
 216 $1.645 \cdot \sigma$) in λ_{amip} is almost the same size as the spread in λ_{4xCO2} (Table 1). The spread in
 217 EffCS_{amip} is narrower primarily because λ_{amip} is on average more negative than λ_{4xCO2} . Since
 218 EffCS depends on the reciprocal of λ , the same spread in λ , shifted to more negative
 219 numbers, will give rise to a narrower spread in EffCS (e.g., Roe, 2009). A similar spread in
 220 in λ_{amip} and λ_{4xCO2} suggests that different patterns of SST change across AOGCMs do not
 221 contribute significantly to the spread in atmospheric feedbacks in abrupt-4xCO2 experiments
 222 (see also Ringer et al., 2014; Andrews and Webb, 2018), which must therefore come about
 223 due to differences in atmospheric physics and parameterisations.

224

225 EffCS_{4xCO2} (of the parent AOGCM) is in all cases larger than EffCS_{amip} , ranging from 2.4 to
 226 4.6K (Table 1). In the multi-model-mean, EffCS_{4xCO2} is $\sim 67\%$ larger than that implied from
 227 EffCS_{amip} . This model-mean historical pattern effect is substantially larger than the 26%
 228 found by Armour (2017), supporting the hypothesis that the pattern effect is larger in the
 229 historical record than simulated in transient 1%CO₂ AOGCM simulations because the later
 230 miss key features of the observed warming pattern. This result is even more striking given
 231 that Armour (2017) used an EffCS definition from abrupt-4xCO2 that gives larger values than
 232 ours (they used years 21-150 of abrupt-4xCO2, whereas we use years 1-150).

233

234 It is also useful to study shorter time periods to help inform our understanding of the
 235 relationship between shorter term variations in temperature and radiative fluxes, as have
 236 been used by many studies to estimate EffCS particularly since the satellite era (e.g. Forster,
 237 2017). Figure 2f shows the feedback parameter for 30yr moving windows over the historical
 238 period in the AGCM simulations (calculated as per Gregory and Andrews, 2016), in
 239 comparison to $\lambda_{4\times\text{CO}_2}$ (horizontal lines). There is substantial multi-decadal variability in the
 240 feedback parameter that is common to all models, with a peak in feedback parameter
 241 (higher EffCS) around the 1940s and a minimum (lower EffCS) in the most recent decades
 242 (post ~1980). Generally λ_{amip} is always more negative than $\lambda_{4\times\text{CO}_2}$. There are only a few
 243 instances where the λ_{amip} is similar to $\lambda_{4\times\text{CO}_2}$, for example ~1940 for HadGEM2 and GFDL-
 244 AM2.1, but no instances where λ_{amip} is substantially less negative than $\lambda_{4\times\text{CO}_2}$. The difference
 245 is greatest in the most recent decades, suggesting that energy budget constraints on ECS
 246 based on recent decades of satellite data will be most strongly biased low. This is consistent
 247 with process understanding of the pattern effect, since recent decades have shown
 248 substantial cooling in the eastern Pacific and Southern Ocean while warming in the west
 249 Pacific warm pool (e.g. Zhou et al., 2016). The cooling in the descent region of the tropical
 250 Pacific will favour increased cloudiness (a negative feedback), while warming in the west
 251 Pacific ascent region efficiently warms free tropospheric air (increasing the negative lapse-
 252 rate feedback widely across the tropics and mid-latitudes) as well as further increasing the
 253 lower tropospheric stability and cloudiness in the marine low-cloud descent regions (Zhou et
 254 al., 2016; Ceppi and Gregory, 2017; Andrews and Webb, 2018).

255

256 Most of the multi-decadal variation in feedback strength comes from changes in the strength
 257 of cloud feedback (the correlation between the Net and CRE feedback timeseries, calculated
 258 in a similar way, is >0.94 in each AGCM) while the clear-sky feedbacks show less variation
 259 (not shown). This, as well as atmospheric variability, helps explain why cloud feedback is not
 260 as linearly correlated to dT variations over the full historical period compared to clear-sky
 261 feedbacks ($r=0.48$ for CRE compared to 0.99 and 0.93 for the clear-sky fluxes, Figures
 262 1d,e,f).

263 4. Constraints on observed estimates of climate 264 sensitivity

265 The pattern effect causing the difference between simulated EffCS under historical climate
 266 change and long-term CO_2 increase implies that historical energy budget constraints on

267 EffCS do not directly apply to long-term ECS. To account for this, we use the difference in λ
 268 between amip-piForcing and abrupt-4xCO₂ as a measure of the pattern effect to update
 269 historical energy budget estimates of λ and EffCS. This is in contrast to Armour (2017) who
 270 had to use 1%CO₂ simulations as a surrogate for historical climate change. Here we are
 271 quantifying the pattern effect associated with patterns of temperature change that actually
 272 occurred in the real world, relative to those simulated by AOGCMs to long-term CO₂
 273 increases. The pattern effect therefore assumes that long-term warming patterns in
 274 AOGCMs not yet seen in the historical record, and the radiative response to them, are
 275 credible (see Discussion).

276

277 To illustrate the impact of the pattern effect we use the Otto et al. (2013) historical energy
 278 budget constraints as our starting point, though other datasets exist (see Forster, 2017) and
 279 clearly the EffCS estimates presented below will depend on this. First, we reproduce the
 280 historical EffCS estimates reported in Otto et al. (2013) using their best estimate and 5-95%
 281 confidence intervals for the historical (denoted by subscript 'hist') change in temperature
 282 ($dT_{\text{hist}}=0.48\pm 0.2$ K), heat uptake ($dN_{\text{hist}}=0.35\pm 0.13$ Wm⁻²) and radiative forcing
 283 ($dF_{\text{hist}}=1.21\pm 0.52$ Wm⁻²) for the 40 yr period 1970-2009 relative to pre-industrial (which they
 284 define as 1860-1879) (their Table S1, row 5). To be consistent with Otto et al. (2013) we also
 285 use their forcing and its uncertainty for a doubling of CO₂ ($F_{2x}=3.44$ ($\pm 10\%$) Wm⁻²). We
 286 randomly sample (with replacement) 10 million times from the gaussian distributions of dT_{hist} ,
 287 dN_{hist} , dF_{hist} and F_{2x} to calculate $\lambda_{\text{hist}}=(dN_{\text{hist}}-dF_{\text{hist}})/dT_{\text{hist}}$ and $\text{EffCS}_{\text{hist}}=-F_{2x}/\lambda_{\text{hist}}$. We assume
 288 the uncertainty in F_{2x} and the greenhouse gas component of dF_{hist} are correlated as in Otto et
 289 al. (2013). The resulting EffCS values are binned into intervals of 0.02 and normalised to
 290 produce a probability density function (PDF), excluding values less than zero and greater
 291 than twenty. The resulting PDF and percentiles (Figure 3, black lines) recovers the Otto et al.
 292 (2013) $\text{EffCS}_{\text{hist}}$ median (1.9K) and 5-95% confidence interval (0.9-5.0K) to within 0.1K.

293

294 Following Armour (2017), we update the Otto et al. (2013) EffCS estimate for the pattern
 295 effect between historical climate change and abrupt-4xCO₂ using two methods. We first
 296 scale the historical feedback parameter λ_{hist} by the ratio of the feedbacks found in the amip-
 297 piForcing and abrupt-4xCO₂ simulations, so $\lambda=\lambda_{\text{hist}}*S$ where $S=\lambda_{4x\text{CO}_2}/\lambda_{\text{amip}}$ (Table 1). EffCS is
 298 then given by $\text{EffCS}=-F_{2x}/\lambda=-F_{2x}/(\lambda_{\text{hist}}*S)$ (equivalent to Equation 4 in Armour 2017).

299 Alternatively, we update λ_{hist} by the difference in feedbacks, according to $\lambda=\lambda_{\text{hist}}+\Delta\lambda$, where
 300 $\Delta\lambda=\lambda_{4x\text{CO}_2}-\lambda_{\text{amip}}$. EffCS is then given by $\text{EffCS}=-F_{2x}/\lambda=-F_{2x}/(\lambda_{\text{hist}}+\Delta\lambda)$ (equivalent to Equation 5
 301 in Armour 2017). We then calculate the EffCS PDF as above by randomly sampling from
 302 the F_{2x} and λ_{hist} distributions, along with S and $\Delta\lambda$ chosen randomly with equal likelihood from
 303 the individual model results (Table 1). Note that using the difference ($\Delta\lambda$) approach

304 increases the likelihood of returning very large (or even negative) EffCS values, since
305 $\lambda = \lambda_{\text{hist}} + \Delta\lambda$ can result in λ values close to zero or even with a changed sign when sampling
306 λ_{hist} values that are small. Hence the results of this method are potentially sensitive to the
307 assumption of excluding negative EffCS values or those greater than 20K.

308
309 We compare the PDF of EffCS_{hist} (which is an approximation of Otto et al. (2013)) against its
310 updated versions that accounts of the pattern effect in Figure 3. The Otto et al. (2013)
311 median and 5-95% confidence interval increases from 1.9K (0.9-5.0K) to 3.2K (1.5-8.1K)
312 using the ratio (S) approach (Figure 3, red lines), or 2.7K (1.1-10.2K) if we use the difference
313 ($\Delta\lambda$) approach (Figure 3, blue lines). Alternatively, if we take the Otto et al. (2013) data
314 relating to their most recent decade (2000-2009) (their Table S1 row 4) then the Otto et al.
315 (2013) estimate and 5-95% confidence interval increases from 2.0K (1.2-3.9K) to 3.3K (1.8-
316 6.8K) using the ratio approach or 3.0K (1.5-9.7K) using the difference approach. Thus,
317 eitherway and for different time periods, the pattern effect from amip-piForcing to abrupt-
318 4xCO₂ results in a substantial median ECS increase, while the lowest values of ECS
319 become less likely, and higher ECS values become much harder to rule out.

320
321 Another way of estimating the pattern effect is by comparing feedbacks in AOGCM historical
322 simulations to abrupt-4xCO₂ (e.g. Paynter and Frolicher, 2015; Marvel et al., 2018).
323 However we believe amip-piForcing is superior, because (i) the diagnosed pattern effect in
324 an AOGCM historical simulation will depend on its ability to correctly simulate the patterns of
325 historical climate change, including the magnitude and timing of unforced variability, which
326 they are not expected to simulate correctly (e.g. Zhou et al., 2016; Mauritsen, 2016) and (ii)
327 determining feedbacks in AOGCM historical simulations requires knowledge of the time-
328 varying effective radiative forcing of the model, something which is not routinely diagnosed
329 and is difficult to assume because of model diversity in forcing, particularly from aerosols
330 (Forster, 2017). The amip-piForcing approach alleviates both of the above issues.

331
332 Note that for simplicity in the above calculations we have assumed that λ_{amip} (calculated via
333 linear regression over the amip-piForcing simulations, Section 3) is appropriate to the time
334 periods and methodology of Otto et al. (2013) (who use finite differences, rather than linear
335 regression, between decades to calculate changes). To check this we recompute λ_{amip} and
336 the corresponding S and $\Delta\lambda$ values using the same method and time-periods as Otto et al.,
337 i.e. $\lambda_{\text{amip}} = dN/dT$, where dN and dT are averaged over the relevant decades (though for 2000-
338 2009 we use the 1995-2004 decade, since the GFDL runs finished in 2004). We cannot use
339 an identical baseline as Otto et al. (2013) since our simulations begin in 1871 and their
340 baseline begins in 1860. Regardless, for 1979-2009 or 2000-2009, the resulting updated

341 EffCS PDF has a median and 5-95% confidence interval to within $\pm 15\%$ of the regression
342 methods used above. Hence in practice our conclusions are not sensitive on this
343 assumption.

344 5. Summary and discussion

345 An intercomparison of AGCMs forced with historical (post 1870) sea-surface-temperatures
346 and sea-ice from the AMIP II boundary condition dataset reveal some common results:

347

348 1. When AGCMs are forced with historical SST and sea-ice changes the models agree
349 on an effective climate sensitivity (EffCS) of $\sim 2\text{K}$, in line with best estimates from
350 historical energy budget variations (e.g. Otto et al., 2013) but significantly lower than
351 the EffCS of the corresponding parent AOGCMs when forced with abrupt-4xCO₂
352 ($\sim 2.4 - 4.6\text{K}$ for the corresponding set of models).

353

354 2. The lower historical EffCS relative to abrupt-4xCO₂ is predominantly because LW
355 clear-sky and cloud radiative feedbacks are less positive in response to historical
356 SST and sea-ice variations than in long-term climate sensitivity simulations. This is
357 an example of what is called a 'pattern effect' (Stevens et al., 2016), and is consistent
358 with process understanding that suggests lapse-rate and low-cloud feedbacks vary
359 most with SST patterns, especially those in the tropical Pacific ascent/descent
360 regions which have large impacts on atmospheric stability (Zhou et al., 2016; Ceppi
361 and Gregory, 2017, Andrews and Webb, 2018).

362

363 3. The models agree that the most recent decades (e.g. 1980-2010) generally give rise
364 to the most negative feedbacks (lowest EffCS). Hence the pattern effect will be
365 largest for estimates of feedbacks and EffCS based on the satellite era. This is a
366 period when the eastern tropical Pacific and Southern Ocean, regions important for
367 the pattern effect, have been cooling, but are not expected to continue to do so in the
368 long-term response to increased CO₂ (e.g. Zhou et al., 2016).

369

370 The pattern effect causing the difference between EffCS under historical climate change and
371 long-term CO₂ changes implies that current constraints on climate sensitivity that do not
372 consider this give values that are too low and are overly constrained, particularly at the
373 upper bound. We present an approach to adjust historical energy budget derived EffCS
374 estimates for the pattern effect. For example, the historical (1860-1879 to 1970-2009)

375 observational EffCS estimate (median) and 5-95% confidence interval of Otto et al. (2013)
376 increases from 1.9K (0.9-5.0K) to 3.2K (1.5-8.1K) using an approach that scales the
377 historical feedback parameter by the ratio of the feedbacks found in amip-piForcing and
378 abrupt-4xCO₂. Thus the pattern effect increases historical EffCS median values, reduces
379 the likelihood of the lowest EffCS values, and makes higher values significantly harder to
380 rule out. Determining whether values towards the extremes of these bounds are plausible
381 would require further understanding of the pattern effect or assessing and combining other
382 lines of evidence, such as from process understanding (see Stevens et al., 2016). This is
383 important because a higher EffCS increases the risk of state-dependent feedbacks and large
384 warmings (Bloch-Johnson et al., 2015).

385

386 The pattern effect between historical climate change and long-term CO₂ increase assumes
387 that key aspects of long-term warming patterns simulated by AOGCMs not yet seen in the
388 observational record, such as substantial warming of the Southern Ocean and eastern
389 tropical Pacific, and the radiative response to them, are credible. Such patterns are
390 consistent with paleo records (e.g. Masson-Delmotte et al. 2013; Fedorov et al., 2015) and
391 basic physical understanding of the behaviour and timescale of oceanic upwelling (e.g.
392 Clement et al. 1996, Held et al., 2010; Armour et al., 2016), though they are difficult to
393 observationally constrain (Mauritsen, 2016). To argue for a negligible pattern effect (e.g.
394 Lewis and Curry, 2018) would require that atmospheric feedbacks are insensitive to patterns
395 of temperature change, or that the pattern of observed historical temperature change
396 represents the equilibrated pattern response to increased CO₂. This is at odds with basic
397 physical understanding and bodies of work on the role for unforced variability, transient
398 effects and non-CO₂ forcings such as aerosols on the pattern of historical climate change
399 (e.g. Held et al., 2010; Jones et al., 2013; Xie et al., 2016; Takahasi and Watanabe, 2016;
400 Armour et al., 2016). Further progress in constraining the pattern effect and EffCS will come
401 from improved understanding of the causes and processes of surface temperature change
402 patterns in observations and AOGCM projections, as well as the radiative response to them.

403 Acknowledgments and data

404 Global-annual timeseries data of temperature and radiative flux change in the amip-
405 piForcing simulations, as well as the abrupt-4xCO₂ simulations not in the CMIP5 archive,
406 are provided in the Supporting Datasets. We thank Michael Winton, Tom Knutson, Mark
407 Ringer, Gareth Jones and two anonymous reviewers for constructive comments. TA, JMG

408 and MJW were supported by the Met Office Hadley Centre Climate Programme funded by
409 BEIS and Defra.. PMF was supported by grant NE/N006038/1.

410 References

- 411 Andrews, T., and M.J. Webb, 2018: The dependence of global cloud and lapse rate
412 feedbacks on the spatial structure of tropical pacific warming. *J. Climate*, 31, 641–654,
413 doi:10.1175/JCLI-D-17-0087.
- 414
- 415 Andrews, T., J.M. Gregory, and M.J. Webb, 2015: The dependence of radiative forcing and
416 feedback on evolving patterns of surface temperature change in climate models, *J. Clim.*, 28,
417 1630–1648, doi:10.1175/jcli-d-14-00545.1.
- 418
- 419 Andrews, T., 2014: Using an AGCM to diagnose historical effective radiative forcing and
420 mechanisms of recent decadal climate change, *J. Clim.*, 27, 1193–1209, doi:10.1175/jcli-d-
421 13-00336.1.
- 422
- 423 Andrews, T., J.M. Gregory, M.J. Webb, and K.E. Taylor, 2012: Forcing, feedbacks and
424 climate sensitivity in CMIP5 coupled atmosphere–ocean climate models, *Geophys. Res.*
425 *Let.*, 39, L09712.
- 426
- 427 Armour, K.C., 2017: Energy budget constraints on climate sensitivity in light of inconstant
428 climate feedbacks, *Nature Climate Change*, 7, 331–335, doi:10.1038/nclimate3278.
- 429
- 430 Armour, K.C., J. Marshall, J.R. Scott, A. Donohoe and E.R. Newsom, 2016: Southern
431 Ocean warming delayed by circumpolar upwelling and equatorward transport. *Nature*
432 *Geoscience*, 9, 549–554, doi:10.1038/ngeo2731.
- 433
- 434 Armour, K.C., C.M. Bitz and G.H. Roe, 2013: Time-varying climate sensitivity from regional
435 feedbacks. *J. Climate*, 26, 4518–4534, doi: 10.1175/JCLI-D-12-00544.1.
- 436
- 437 Bloch-Johnson, J., R.T. Pierrehumbert, and D S. Abbot, 2015: Feedback temperature
438 dependence determines the risk of high warming. *Geophys. Res. Let.*, 42, 4973–4980. doi:
439 10.1002/2015GL064240.
- 440

- 441 Ceppi, P., and J.M. Gregory, 2017: Relationship of tropospheric stability to climate sensitivity
442 and Earth's observed radiation budget. PNAS, 114(50), doi:10.1073/pnas.1714308114.
443
- 444 Clement, A.C., R. Seager, M.A. Cane and S.E. Zebiak (1996), An ocean dynamical
445 thermostat. J. Climate, 9, 2190–2196.
446
- 447 Collins, M., et al. (2013), Long-term climate change: Projections, commitments and
448 irreversibility, in Climate Change 2013: The Physical Science Basis. Contribution of Working
449 Group I to the Fifth Assessment Report of the Intergovernmental Panel on Climate Change,
450 edited by M. Collins et al., pp. 1029–1136, Cambridge Univ. Press.
451
- 452 Fedorov, A.V., N.J. Burls, K.T. Lawrence and L.C. Peterson, 2015: Tightly linked zonal and
453 meridional sea surface temperature gradients over the past five million years. Nature
454 Geoscience, 8, 975-980, doi:10.1038/ngeo2755.
455
- 456 Forster, P.M., 2017: Inference of Climate Sensitivity from Analysis of Earth's Energy Budget,
457 Annu. Rev. Earth Planet. Sci., 44, 85-106. doi: 10.1146/annurev-earth-060614-105156.
458
- 459 Gates, W.L., et al., 1999: An Overview of the Results of the Atmospheric Model
460 Intercomparison Project (AMIP I). Bull. Amer. Meteor. Soc., 80, 29–56.
461
- 462 Gregory, J.M., and T. Andrews, 2016: Variation in climate sensitivity and feedback
463 parameters during the historical period. Geophys. Res. Lett., 43, 3911–3920,
464 doi:10.1002/2016GL068406.
465
- 466 Gregory, J.M., R.J. Stouffer, S.C. Raper, P.A. Stott, and N.A. Rayner, 2002: An
467 Observationally Based Estimate of the Climate Sensitivity. J. Climate, 15, 3117–3121.
468
- 469 Haugstad, A. D., K. C. Armour, D. S. Battisti, and B. E. J. Rose (2017), Relative roles of
470 surface temperature and climate forcing patterns in the inconstancy of radiative feedbacks,
471 Geophys. Res. Lett., 44, 7455–7463, doi:10.1002/2017GL074372.
472
- 473 Held, I.M., et al. (2010), Probing the fast and slow components of global warming by returning
474 abruptly to preindustrial forcing. J. Climate, 23, 2418-2427.
475

- 476 Hurrell, J., J. Hack, D. Shea, J. Caron, and J. Rosinski, 2008: A New Sea Surface
477 Temperature and Sea Ice Boundary Dataset for the Community Atmosphere Model. *J.*
478 *Climate*, 21, 5145–5153, doi: 10.1175/2008JCLI2292.1.
- 479
- 480 Jones, G. S., P. A. Stott, and N. Christidis (2013), Attribution of observed historical near-
481 surface temperature variations to anthropogenic and natural causes using CMIP5
482 simulations, *J. Geophys. Res. Atmos.*, 118, 4001–4024, doi: 10.1002/jgrd.50239.
- 483
- 484 Lewis, N. and J. Curry, 2018: The Impact of Recent Forcing and Ocean Heat Uptake Data
485 on Estimates of Climate Sensitivity. *J. Climate*, 31, 6051–6071, doi:10.1175/JCLI-D-17-
486 0667.1.
- 487
- 488 Marvel, K., Pincus, R., Schmidt, G. A., & Miller, R. L. (2018). Internal variability and
489 disequilibrium confound estimates of climate sensitivity from observations. *Geophysical*
490 *Research Letters*, 45, 1595–1601. <https://doi.org/10.1002/2017GL076468>.
- 491
- 492 Masson-Delmotte, V., et al. (2013), Information from paleoclimate archives, in *Climate*
493 *Change 2013: The Physical Science Basis. Contribution of Working Group I to the Fifth*
494 *Assessment Report of the Intergovernmental Panel on Climate Change*, edited by M. Collins
495 et al., pp. 383–464, Cambridge Univ. Press.
- 496
- 497 Mauritsen, T., et al., 2018: Developments in the MPI-M Earth System Model version 1.2
498 (MPI-ESM1.2) and its response to increase CO₂. Submitted to JAMES.
- 499
- 500 Mauritsen, T., 2016: Global warming: Clouds cooled the Earth. *Nat. Geosci.*, 9, 865-867,
501 doi:10.1038/ngeo2838.
- 502
- 503 Otto., A., et al., 2013: Energy budget constraints on climate response. *Nature Geoscience*.
504 6, 415-416, doi:10.1038/ngeo1836.
- 505
- 506 Paynter, D., Frölicher, T. L., Horowitz, L. W., & Silvers, L. G. (2018). Equilibrium climate
507 sensitivity obtained from multimillennial runs of two GFDL climate models. *Journal of*
508 *Geophysical Research: Atmospheres*, 123, 1921–1941. doi:10.1002/2017JD027885.
- 509
- 510 Paynter, D., and T. L. Frölicher (2015), Sensitivity of radiative forcing, ocean heat uptake,
511 and climate feedback to changes in anthropogenic greenhouse gases and aerosols, *J.*
512 *Geophys. Res. Atmos.*, 120, 9837–9854, doi:10.1002/2015JD023364.

513

514 Proistosescu, C., and P.J. Huybers, 2017: Slow climate mode reconciles historical and
515 model-based estimates of climate sensitivity. *Sci. Adv.*, 3, 7, doi:10.1126/sciadv.1602821.

516

517 Roe, G., 2009: Feedbacks, timescales, and seeing red. *Annu. Rev. Earth Planet. Sci.*, 37:93-
518 115: doi: 10.1146/annurev.earth.061008.134734.

519

520 Rose, B.E.J., K.C. Armour, D.S. Battisti, N. Feldl, and D.D.B. Koll, 2014: The dependence of
521 transient climate sensitivity and radiative feedbacks on the spatial pattern of ocean heat
522 uptake, *Geophys. Res. Lett.*, 41, 1071–1078, doi:10.1002/2013GL058955.

523

524 Ringer, M.A., T. Andrews and M.J. Webb, 2014: Global-mean radiative feedbacks and
525 forcing in atmosphere-only and fully-coupled climate change experiments. *Geophys. Res.*
526 *Lett.*, 41, 4035-4042, doi:10.1002/2014GL060347.

527

528 Senior, C.A., and J.F.B Mitchell, 2000: The time-dependence of climate sensitivity.
529 *Geophys. Res. Lett.*, 21(17), 2685-2688, doi:10.1029/2000GL011373.

530

531 Silvers, L.G., D. Paynter and M. Zhao, 2018: The diversity of cloud responses to twentieth
532 century sea surface temperatures. *Geophysical Research Letters*, 45, 391–400.
533 <https://doi.org/10.1002/2017GL075583>.

534

535 Smith, D.M., B.B.B. Booth, N.J. Dunstone, R. Eade, L. Hermanson, G.S. Jones, A.A Scaife,
536 K.L. Sheen and V. Thompson, 2016: Role of volcanic and anthropogenic aerosols in the
537 recent global surface warming slowdown. *Nature Climate Change*. 6, 936-940,
538 doi:10.1038/nclimate3058.

539

540 Stevens, B., S.C. Sherwood, S. Bony, S. and M.J. Webb, 2016: Prospects for narrowing
541 bounds on Earth's equilibrium climate sensitivity. *Earth's Future*, 4: 512-522.
542 doi:10.1002/2016EF000376.

543

544 Takahashi, C., and M. Watanabe, 2016: Pacific trade winds accelerated by aerosol forcing
545 over the past two decades. *Nature Climate Change*, 6, 768-772, doi:10.1038/nclimate2996.

546

547 Taylor, K. E., R. J. Stouffer, and G. A. Meehl, 2012: An overview of CMIP5 and the
548 experiment design, *Bull. Am. Meteorol. Soc.*, 93, 485–498, doi:10.1175/bams-d-11-00094.1.

549

- 550 Taylor, K.E., D. Williamson, and F. Zwiers, 2000: The sea surface temperature and sea-ice
551 concentration boundary conditions for AMIP II simulations, PCMDI Report No. 60, Program
552 for Climate Model Diagnosis and Intercomparison, Lawrence Livermore National Laboratory.
553
- 554 Titchner, H. A., and N. A. Rayner (2014), The Met Office Hadley Centre sea ice and sea
555 surface temperature data set, version 2: 1. Sea ice concentrations, *J. Geophys. Res.*
556 *Atmos.*, 119, 2864–2889, doi:10.1002/2013JD020316.
557
- 558 Webb, M.J., et al., 2017: The Cloud Feedback Model Intercomparison Project (CFMIP)
559 contribution to CMIP6. *Geosci. Model Dev.*, 10, 359-384, doi:10.5194/gmd-10-359-2017.
560
- 561 Xie., S-P., Y. Kosaka, and Y.M. Okumura, 2016: Distinct energy budgets for anthropogenic
562 and natural changes during global warming hiatus. *Nature Geoscience*. 9, 29-33,
563 doi:10.1038/ngeo2581.
564
- 565 Zhou, C., M. D. Zelinka, and S. A. Klein, 2017: Analyzing the dependence of global cloud
566 feedback on the spatial pattern of sea surface temperature change with a Green's function
567 approach. *J. Adv. Model. Earth Syst.*, 9, doi:10.1002/2017MS001096.
568
- 569 Zhou., C., M.D. Zelinka and S.A. Klein, 2016: Impact of decadal cloud variations on the
570 Earth's energy budget. *Nature Geoscience*, 9, 871-874, doi:10.1038/ngeo2828.

571 Tables

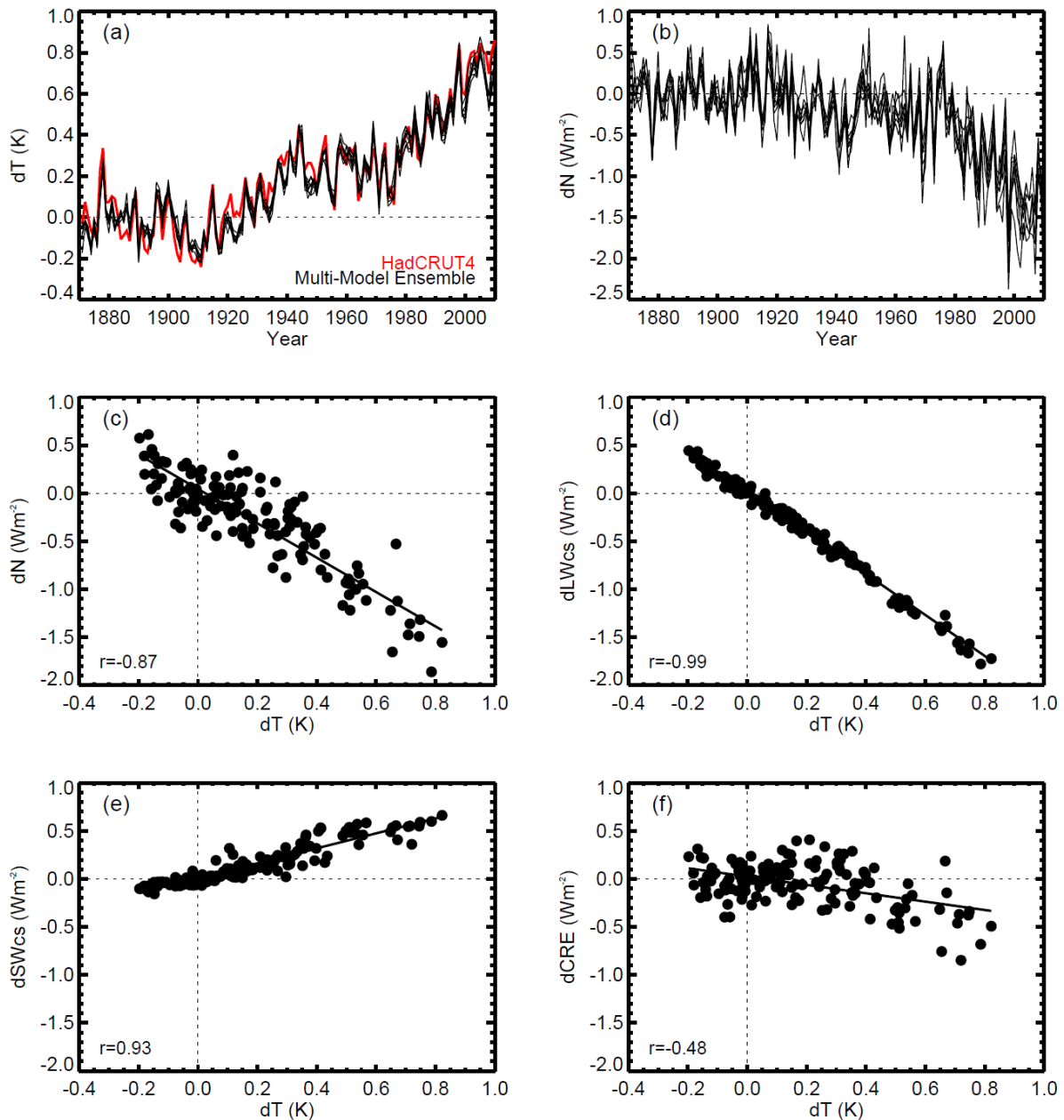
572

	λ_{amip}	$\lambda_{4x\text{CO}_2}$	$S=\lambda_{4x\text{CO}_2}/\lambda_{\text{amip}}$	$\Delta\lambda=\lambda_{4x\text{CO}_2} - \lambda_{\text{amip}}$	$\text{EffCS}_{\text{amip}}$	$\text{EffCS}_{4x\text{CO}_2}$
	($\text{Wm}^{-2} \text{K}^{-1}$)	($\text{Wm}^{-2} \text{K}^{-1}$)		($\text{Wm}^{-2} \text{K}^{-1}$)	(K)	(K)
CAM4	-2.27	-1.23	0.54	1.04	1.57	2.90
CAM5.3	-1.71	n/a	n/a	n/a	n/a	n/a
ECHAM6.3	-1.90	-1.36	0.72	0.54	2.17	3.01
GFDL-AM2.1	-1.67	-1.38	0.83	0.29	2.01	2.43
GFDL-AM3	-1.40	-0.75	0.53	0.65	2.13	3.99
GFDL-AM4.0	-1.91	n/a	n/a	n/a	n/a	n/a
HadAM3	-1.65	-1.04	0.63	0.61	2.14	3.38
HadGEM2	-1.37	-0.64	0.47	0.73	2.14	4.58
Mean(1.645σ)	-1.74(0.48)	-1.07(0.52)	0.62(0.22)	0.64(0.40)	2.03(0.38)	3.38(1.29)

573

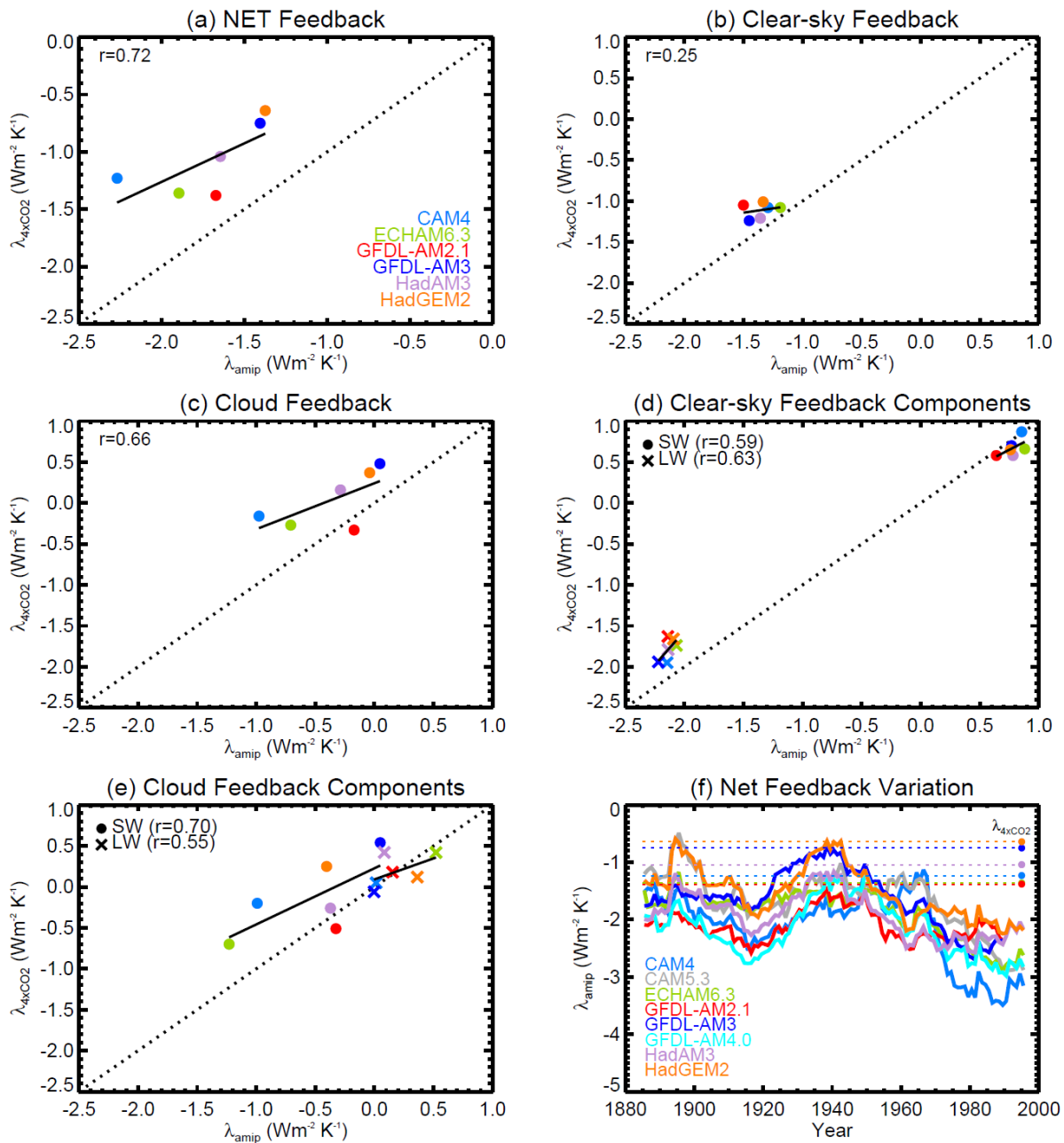
574 **Table 1: Feedback parameters in amip-piForcing (λ_{amip}) and abrupt-4xCO₂ ($\lambda_{4x\text{CO}_2}$)**
575 **AGCM and AOGCM experiments. S and $\Delta\lambda$ are the ratio and differences between**
576 **$\lambda_{4x\text{CO}_2}$ and λ_{amip} respectively. These are used to update feedback parameters derived**
577 **from historical energy budget changes to account for the pattern effect between**
578 **historical climate change and abrupt-4xCO₂. $\text{EffCS}_{\text{amip}}=-F_{2x}/\lambda_{\text{amip}}$ and $\text{EffCS}_{4x\text{CO}_2}=-$**
579 **$F_{2x}/\lambda_{4x\text{CO}_2}$ are the effective climate sensitivities from the amip-piForcing and abrupt-**
580 **4xCO₂ experiments, where F_{2x} is the models effective radiative forcing for a doubling**
581 **of CO₂ (calculated from the abrupt-4xCO₂ experiments using a linear regression**
582 **technique as per Andrews et al., 2012).**

583 Figures



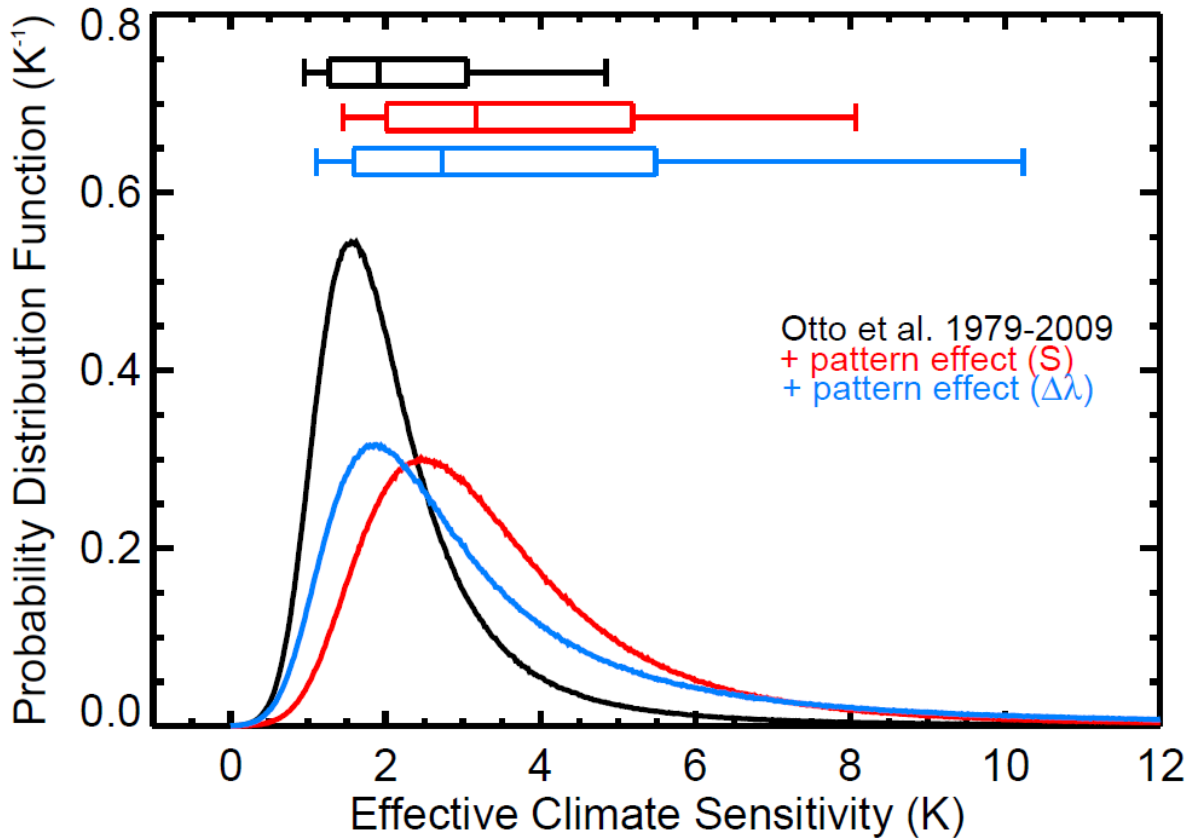
584

585 **Figure 1: (a) Comparison of historical near-surface-air-temperature change (dT)**586 **simulated by the AGCMs in amip-piForcing (individual black lines) against observed**587 **(HadCRUT4) variations (red). (b) Timeseries of the change in net TOA radiative flux**588 **(dN) in the individual AGCM experiments. (c - f) The relationship and correlation**589 **coefficient (r) between the multi-model ensemble-mean (c) dN , (d) LW clear-sky**590 **radiative flux change, $dLWcs$, (e) SW clear-sky radiative flux change, $dSWcs$, and (f)**591 **cloud radiative effect change, $dCRE$, against dT . All points are global-annual-means**592 **covering the historical period (1871-2010) and fluxes are positive downwards.**593 **Changes are relative to an 1871-1900 baseline.**



594

595 **Figure 2: Relationship between the feedback parameter evaluated by regression of dN**
 596 **against dT over the historical period (1871-2010) in amip-piForcing (λ_{amip}) and 150yrs**
 597 **of abrupt-4xCO₂ (λ_{4xCO_2}) for (a) NET radiative feedback, (b) Clear-sky component, (c)**
 598 **CRE component, (d) LW and SW clear-sky components, (e) LW and SW CRE**
 599 **components. (f) Timeseries of λ_{amip} for individual AGCMs evaluated by linear**
 600 **regression of dN against dT in a sliding 30 year window in the amip-piForcing**
 601 **experiments, the year represents the centre of the window. Coloured circles in (f) with**
 602 **horizontal lines show the feedback parameter values from abrupt-4xCO₂.**



603

604 **Figure 3: Comparison of the EffCS probability distribution function from a historical**
 605 **energy budget constraint (Otto et al, 2013), before (black) and after (colours)**
 606 **accounting for the pattern effect between historical climate change and abrupt-**
 607 **4xCO₂. ‘Red’ accounts for the pattern effect by scaling the historical feedback**
 608 **parameter λ_{hist} by the ratio ($S=\lambda_{4x\text{CO}_2}/\lambda_{\text{amip}}$) of the feedbacks found in the amip-**
 609 **piForcing and abrupt-4xCO₂ simulations. ‘Blue’ accounts for the pattern effect by**
 610 **adding the difference in feedbacks ($\Delta\lambda=\lambda_{4x\text{CO}_2}-\lambda_{\text{amip}}$) to λ_{hist} (see Section 4 and Table 1).**
 611 **Box plots show the 5-95% confidence interval (end bars), the 17-83% confidence**
 612 **interval (box ends) and the median (line in box).**